

Study of Thermodynamic Parameters for Nano Zinc Sulfate in the Presence of Proline (amino acid) in Mixed MeOH-H₂O Solvents at Different Temperatures

Radwa T.Rashad ^{1,*} , Esam A. Gomaa ² 

¹ Misr Higher Institute for Engineering and Technology, Mansoura, Egypt

² Chemistry Department, Faculty of Science, Mansoura University, 35516-Mansoura, Egypt

* Correspondence: radwa_tarek@engmet.edu.eg (R.T.R.);

Scopus Author ID 2438214000

Received: 18.10.2021; Accepted: 29.11.2021; Published: 17.09.2022

Abstract: A set of conductometric measurements were conducted using zinc sulfate (ZnSO₄) with different percentages of methanol (MeOH) and water in the presence of Proline (ligand) at four temperatures. The present work aims to estimate diverse thermodynamic parameters for nano Zn (II) sulfate alone and with amino acid (H₂Prol) to form complexes in the solutions. All the data for the used electrolytes and ions is very important for analyzing the salt and explaining the different ion-ion and ion-solvent interactions. The isolated metal complexes derived from the interaction of amino acids with Zn (II) are characterized by chemical and physical methods. Based on spectral data (IR, and UV-Vis), a structure for separated solid complexes is presented and magnetic studies. Furthermore, biological activity measurements are executed, which benefits in determining the factors impacting the thermodynamic parameters and physical properties of the formed complexes in the solution.

Keywords: ion-pair association constants; binary mixed solvents; limiting molar conductance; amino acid; zinc sulfate.

© 2022 by the authors. This article is an open-access article distributed under the terms and conditions of the Creative Commons Attribution (CC BY) license (<https://creativecommons.org/licenses/by/4.0/>).

1. Introduction

The human body has a lot of zinc as a trace element, and its molecular formula is fascinating. It is found at the center of many important enzymes' active structures, including carboxypeptidase, carbonic anhydrase, superoxide dismutase (SOD), and alcohol dehydrogenase [1,2]. Zinc is required to maintain the optimal performance of the human body in various processes such as bone growth, cell-mediated immunity, brain function, and tissue evolution [3,4]. Besides, it is needed for applied and theoretical research and is employed in numerous industries [5-7]. Amino acids are fundamental structural units of proteins that have a tremendously chief role in all biological processes. The study of amino acids' thermodynamic specifications and the electrostatics role is crucial for delivering a molecular understanding of how dissimilar residues interact with the solvent or one another. The production of collagen and cartilage requires essential amino acids such as Proline. Proline plays a significant role in sustaining muscle and joint flexibility. Further, it assists in limiting the accompanying symptoms of UV exposure, such as skin aging, sagging, and wrinkling [8-11].

2. Materials and Methods

2.1. Materials.

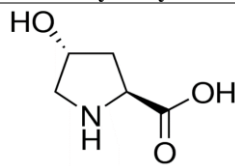
The mixed solvents are synthesized using bidistilled water, which has a specific conductance of 0.09 S cm^{-1} at 298.15 K.

Table 1. The specifications of the chemicals functioned for sample synthesis.

Chemicals	Suppliers	Mass fraction purity	Purification method
Methanol (MeOH)	Sigma-Aldrich	99.5%	None
Zinc sulfate (ZnSO_4)	Sigma-Aldrich	$\geq 99.9\%$	None
Potassium Chloride (KCl)	Sigma-Aldrich	99.9%	None

Tables 1 and 2 show all chemicals and all were exploited without any former purification. The used amino acids (ligands) are (H_2L) supplied from BDH chemicals Ltd as solids. The metal salt used is purchased from Nice Laboratory, India. The water contents were determined through the (Mettler DL 18 Karl Fischer Titrator) and were shown to be smaller than 0.01%. All the glassware was left in the chromic mixture for a day, cleansed many times with distilled water and bidistilled water, then kept in an electric oven to dry. Bidistilled water was obtained by redistilling the ordinary distilled water over KMnO_4 and KOH . The first 25 ml were excluded. Measured specific conductance was found to be $2\text{-}5 \times 10^{-7} \text{ S cm}^{-1}$.

Table 2. Structure and properties of Trans-4-hydroxy Proline.

Properties	Trans-4-hydroxy Proline
Structure of Trans-4-hydroxy proline	
IUPAC name	(2S,4R)-4-hydroxypyrrolidine-2-carboxylic acid
Molar mass	$131.131 \text{ g.mol}^{-1}$
Density	1.907 g/cm^3
Melting point	275°C
Boiling point	Decomposed

2.2. Solutions.

Methanol and water binary mixtures with alcohol mass fractions of 0%, 20%, and 40% were utilized as solvent media in this study. They were created by combining the needed amount of methanol and water (with an error of ± 0.01 percent) according to the continuity formula:

$$\text{Alcohol percentage} = (V_1 d_1) 100 / (V_1 d_1 + V_2 d_2) \quad (1)$$

Where d_1 and d_2 are the relative densities of alcohol and water, alcohol is supplied to water in the amount of V_1 to achieve the required alcohol concentration in V_2 . At temperatures ranging from 298.15 to 313.15 K associated with alcohol mass fractions of 0%, 20%, and 40%, relative permittivity (ϵ), viscosity (η) of (methanol-water), the physical characteristics, and density (ρ) were studied—the equivalent as (with a 5 K step).

2.3. Transmission electron microscope (TEM).

TEM is a widespread device to investigate synthesized solutions' particle size and morphology. TEM provides a decent resolution down to the nanometer scale. Images were acquired using JEOL HRTEM-JEM -2100 (Japan), as shown in Fig 1.

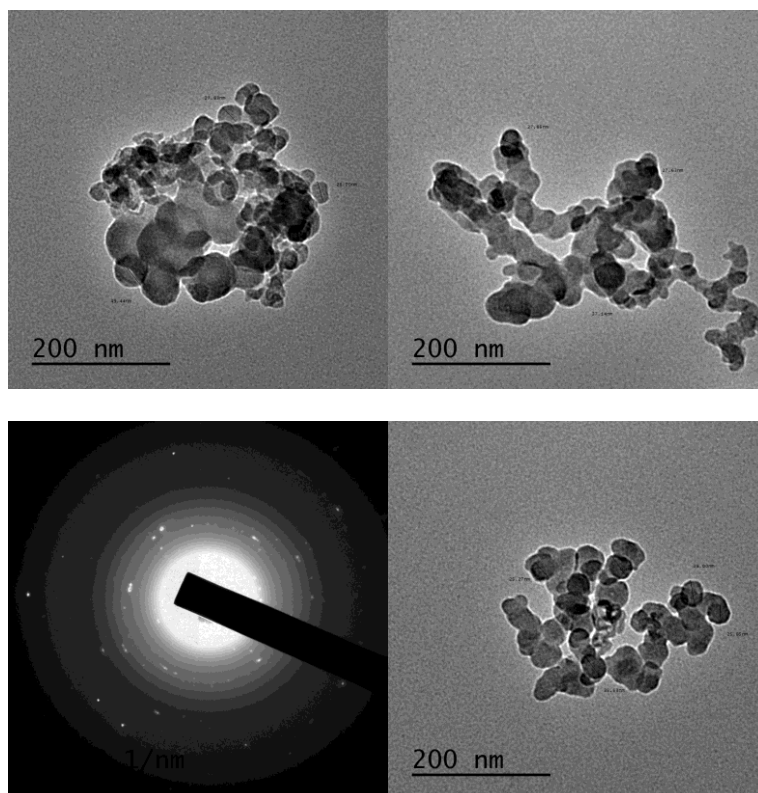


Figure 1. TEM images and electron diffraction of nano zinc sulfate.

2.4. Analysis of complexes.

To suggest the formula of the isolated complexes, elemental analyses are performed. The metal content analyses are carried out according to standard methods [12,13]. i. The divalent metal ions, Zn^{+2} , were determined complexometrically with 0.01 M EDTA using xylenol orange, murexide, or eriochrome black T as an indicator. ii. Elemental analyses (C and H) are carried out in the Microanalytical Unit, Cairo University.

2.5. Working procedure.

2.5.1. Infrared spectra (IR).

The infrared spectra of the studied ligand and its metal complexes were obtained with KBr discs on a Mattson 5000 FTIR spectrometer. At Mansoura University, the spectrum measurement is calibrated using polystyrene film.

2.5.2. Antimicrobial activity.

Gram-positive and Gram-negative bacteria were used to test the compound's antibacterial activity. The compounds' antifungal properties were investigated against (*Candida albicans*). Each chemical was dissolved in DMSO to a concentration of one milligram per milliliter. Autoclave sterilization of 5 cm diameter Whatman filter paper discs manufactured, cut, and sterilized. Agar media containing the complicated solutions was added to Petri plates containing the paper discs, which were then aseptically mounted in the dishes (i.e., beef extract 3 g + agar 20 g + peptone 5 g) inoculated with *Candida albicans*, *Staphylococcus aureus*, and *E. coli*.

The complex's percent activity index was obtained from the following equation:

$$\% \text{ Activity Index} = \frac{\text{Zone of inhibition by test compound (diameter)}}{\text{Zone of inhibition by standard (diameter)}} \times 100 \quad (2)$$

3. Results and Discussion

3.1. Thermodynamic parameters calculations.

Fuoss-Shedlovsky conductivity formulas were used to evaluate the experimental conductance data. In H₂O and (MeOH-H₂O) mixed solvents, the limiting molar conductance (no) of zinc sulfate solutions was established by extrapolating the linear Onsager plot at various temperatures [14-24].

$$\Lambda_m = \frac{(K_s - K_{solv}) \cdot K_{cell} \cdot 1000}{C} \quad (3)$$

Here, K_s and K_{solv} denote the solution's and solvent's specific conductances consecutively; K_{cell} denotes the cell constant, and C denotes the metal salt solution's molar concentration.

$$\frac{1}{\Lambda_m S(Z)} = \frac{1}{\Lambda_o} + \left\{ \frac{KA}{\Lambda_o^2} \right\} (C \Lambda_m \gamma_{\pm}^2 S(Z)) \quad (4)$$

$$S(Z) = 1 + Z + Z^2/2 + Z^3/8 + \dots \text{ etc.} \quad (5)$$

$$Z = \frac{S(\Lambda_m \cdot C)^{1/2}}{\Lambda_o^{3/2}} \quad (6)$$

The value of (Λ_o) was exploited to determine the Onsager slope (S) from Eq. (7)

$$S = a\Lambda_o + b \quad (7)$$

$$a = 8.2 \times 10^5 / (eT)^{3/2} \quad (8)$$

$$b = 82.4 / h((eT)^{1/2}) \quad (9)$$

Where (e) is the solvent's relative permittivity, (η_o) is the solvent's viscosity, and (T) is the temperature. The values of (e) and (o) were used to determine the (S) values. Utilization the data from (Λ_m), S (z), and (Λ_o), the magnitudes of dissociation degrees (K_D) were calculated using the following equation (Eq. (10)):

$$(\alpha) = \Lambda_m S(Z) \Lambda_o \quad \alpha = \Lambda_m S(Z) \Lambda_o \quad (10)$$

The use of these (α) and (e) readings, the mean activity coefficients (γ_{\pm}) were assessed by Eq. (11).

$$\log \gamma_{\pm} = - \frac{Z_+ Z_- A \sqrt{I}}{I + B r^o \sqrt{I}} \quad (11)$$

Where Z₋ and Z₊ are the charges of ions in the solutions A, B delivers the Debye-Hückel constant.

$$A = 1.824 \times 10^6 (eT)^{-3/2} \quad (12)$$

$$B = 50.29 \times 10^8 (eT)^{-1/2} \quad (13)$$

Figures (2-5) show the correlation between molar conductance (Λ_m) and C^{1/2} of nano ZnSO₄ at different temperatures in the absence of ligand

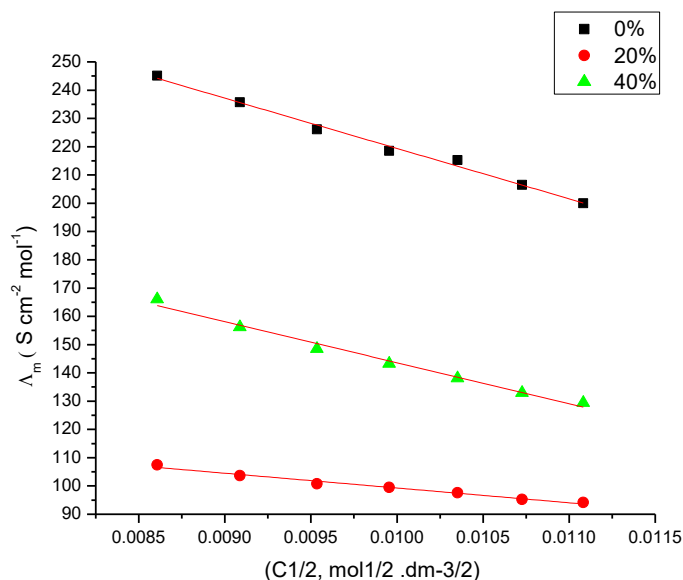


Figure 2. The correlation between molar conductance (Λ_m) and $C^{1/2}$ of nano $ZnSO_4$ at 298.15 K temperature.

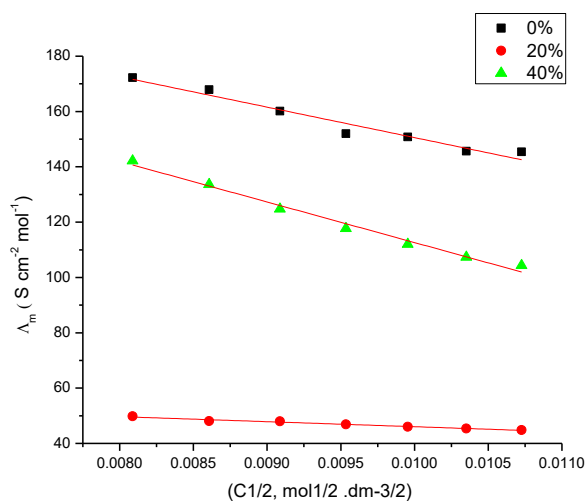


Figure 3. The correlation between molar conductance (Λ_m) and $C^{1/2}$ of nano- $ZnSO_4$ at 303.15 K temperature.

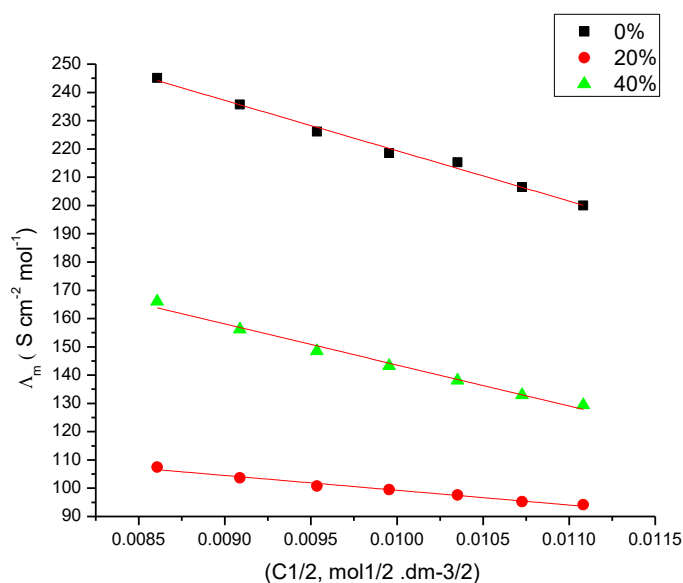


Figure 4. The correlation between molar conductance (Λ_m) and $C^{1/2}$ of nano $ZnSO_4$ at 308.15 K temperature.

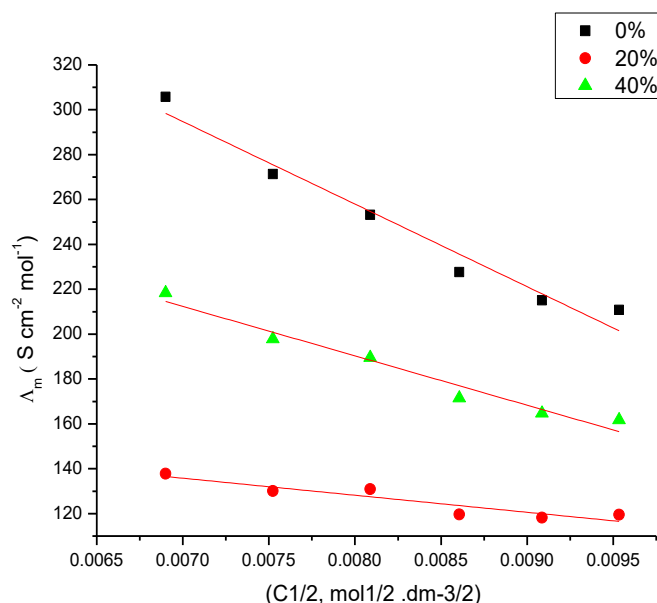


Figure 5. The correlation between molar conductance (Λ_m) and $C^{1/2}$ of nano $ZnSO_4$ at 313.15 K.

Table 3. The mole fractions (X_s), the viscosity, the limiting molar conductance, the molar conductance (Λ_m), the Walden product, the Fuoss-Shedlovsky parameters (S , Z , and $S(z)$), the activity coefficient, and the dissociation constant (K_D) for nano $ZnSO_4$ in a mixed solvent (MeOH- H_2O) are plotted at various temperatures.

T (K)	X_s	$10^3 \eta_o$ (poise)	Λ_o	Λ_m	$\Lambda_o \eta_o$	S	Z	S(z)	γ	$10^3 K_D$
298.15K	0	0.8921	295.35	212.40	2.6348	128.3511	0.0108	1.0109	0.940	1.49
	0.0717	0.9042	125.25	62.45	1.1325	88.7464	0.0147	1.0148	0.951	0.41
	0.1708	0.9209	57.28	31.63	0.5274	75.2427	0.0287	1.0292	0.943	0.58
303.15K	0	0.8001	307.41	215.28	2.4596	139.3559	0.0111	1.0112	0.942	1.33
	0.0717	0.8082	131.34	65.09	1.0619	97.7569	0.0154	1.0155	0.951	0.40
	0.1708	0.8193	61.51	33.01	0.5039	84.3786	0.0296	1.0300	0.943	0.52
308.15K	0	0.7222	306.25	219.65	2.2099	147.8331	0.0121	1.0121	0.941	1.48
	0.0717	0.7329	146.47	67.97	1.0734	109.0197	0.0149	1.0150	0.952	0.33
	0.1708	0.7478	66.47	33.24	0.4970	96.5888	0.0303	1.0307	0.939	0.42
313.15K	0	0.6211	325.34	221.95	2.0206	166.3458	0.0124	1.0125	0.941	1.18
	0.0717	0.6911	153.52	71.99	1.0609	118.4828	0.0155	1.0157	0.949	0.33
	0.1708	0.7092	77.58	35.08	0.5501	105.247	0.0269	1.0272	0.941	0.31

Λ_o in ($S\ cm^2.mol^{-1}$), Λ_m in ($S\ cm^2.mol^{-1}$)

The conductometric thermodynamic parameters for nano $ZnSO_4$ alone in mixed MeOH- H_2O solvents are presented in Table 3, decreasing their values by increasing the methanol favoring less solvation. All the association thermodynamic parameters for nano $ZnSO_4$ are increased with the temperature rise and increased in methanol percentages in the mixture, indicating more interaction by association.

3.2. Free energies of association of nano $ZnSO_4$ in the absence of ligands.

Free energies, enthalpies, the association constants, and entropies of association for nano $ZnSO_4$ at different concentrations of methanol-water at different temperatures are tabulated in Table 4.

Table 4. Association constants, activation energy, enthalpies, and entropies of correlation for nano $ZnSO_4$ at various temperatures in the absence of ligands.

T (K)	X_s	Ea ($kJ.mol^{-1}$)	ΔH_A ($kJ.mol^{-1}$)	$T\Delta S_A$ ($kJ.mol^{-1}$)	ΔS_A ($J.mol^{-1}$)
	0	3.3531	18.4189	34.5292	115.81

T (K)	X _s	E _a (kJ.mol ⁻¹)	ΔH _A (kJ.mol ⁻¹)	TΔS _A (kJ.mol ⁻¹)	ΔS _A (J.mol ⁻¹)
298.15	0.0717	5.2394	21.4143	38.7376	129.92
	0.1708	5.7211	35.1614	53.1398	178.23
303.15	0	3.3531	18.4189	34.8591	114.99
	0.0717	5.2394	21.4143	39.8524	131.46
	0.1708	5.7211	35.1614	54.7414	180.57
308.15	0	3.3531	18.4189	35.1108	113.94
	0.0717	5.2394	21.4143	40.9645	132.74
	0.1708	5.7211	35.1614	55.4636	179.99
313.15	0	3.3531	18.4189	36.0094	114.09
	0.0717	5.2394	21.4143	41.3250	132.96
	0.1708	5.7211	35.1614	55.8179	178.24

The obtained results for nano zinc sulfate in the binary mixed solvent (MeOH-H₂O) at different temperatures are unlike the findings in the case of water.

Zinc sulfate's limiting molar conductance in (MeOH-H₂O) is less than its value in water. This might be regarded as the fact that the conductivity tends to decrease by increasing the mixed solvent. Therefore, a higher reduction is apparent in the 20% and 40% cases, where 40% has the largest reduction. This is due to inter and intra-molecular hydrogen bonds, which hinder the mobility of ions. In this case, raising the methanol content in the solvent promotes a reduction in both solvation and dissociation of the zinc sulfate molecules.

By definition, the correlation constants for nano zinc sulfate in 20% (MeOH-H₂O) are less than those in water. At reduced methanol concentration, the occurring interactions between methanol and The cage-like structure development (often referred to as icebergs) surrounding the methanol hydrophobic ends affects the water. Subsequently, this formation alters the ions' freedom and degree of mobility and limits the association constant.

3.2.1. Association parameters of the nano metals in the presence of ligands (trans-4-hydroxy Proline).

The relation between Λ_m and $C^{1/2}$ for nano ZnSO₄ at various temperatures in the existence of trans-4-hydroxy Proline at (0%, 20%, and 40%) MeOH-H₂O.

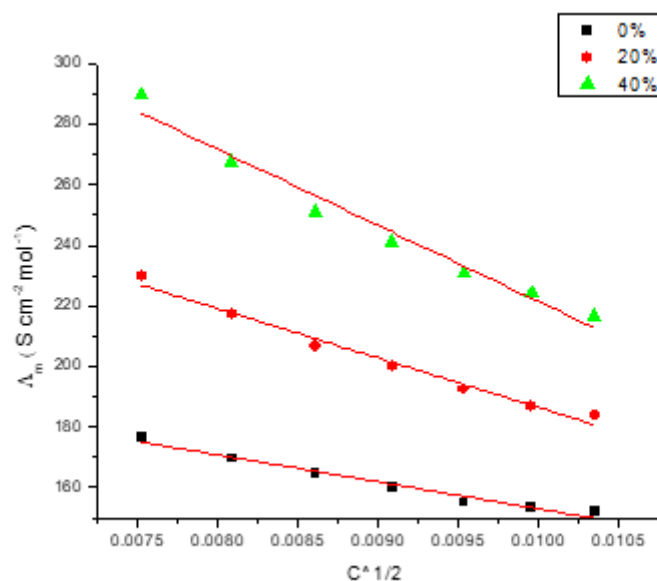


Figure 6. The correlation between (Λ_m) and $C^{1/2}$ of nano ZnSO₄ at (298.15K) temperature.

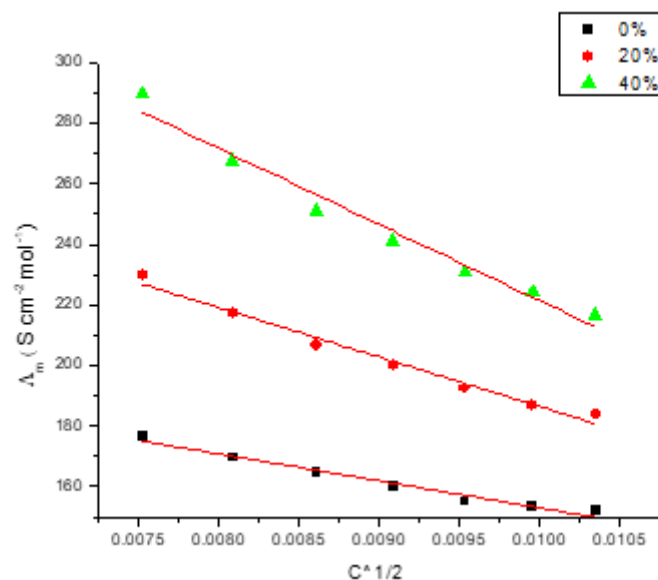


Figure 7. The correlation between (Λ_m) and ($C^{1/2}$) of nano $ZnSO_4$ at (303.15K) temperature.

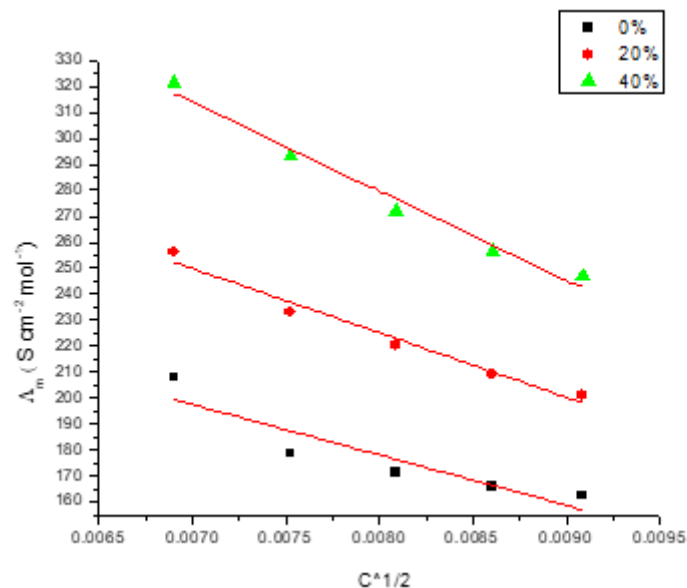


Figure 8. The correlation between (Λ_m) and $C^{1/2}$ of nano $ZnSO_4$ at (308.15K) temperature.

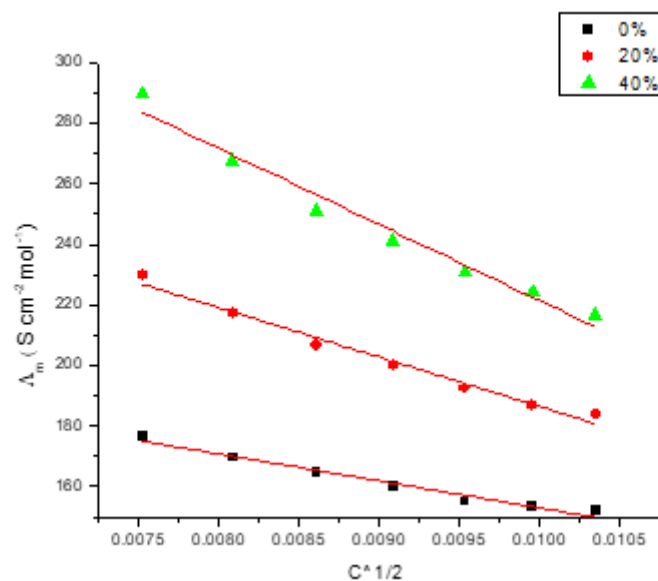


Figure 9. The correlation between (Λ_m) and $C^{1/2}$ of nano $ZnSO_4$ at (313.15K) temperature.

Table 5. The importance of mole fractions (XS), activity coefficient (γ_{\pm}), the values of viscosity (η_0), limiting molar conductance (Λ), molar conductance (Λ_m), Walden product ($\Lambda_0\eta_0$), Fuoss-Shedlovsky parameters (S, Z, and S(z)), and dissociation constant (KD) for nano ZnSO₄ in the existence of trans-4- hydroxyproline in a mixture solution (MeOH-H₂O) at various temperatures.

T K	X _s	10 ² η ₀ (poise)	Λ ₀	Λ _m	Λ ₀ η ₀	S	Z	S(z)	±Y	10 ³ K _D
298.15K	0	0.8921	155.23	93.51	0.9570	85.1164	0.0076	1.0076	0.955	0.62
	0.0717	0.9042	245.11	172.71	0.9571	85.1254	0.0104	1.0105	0.939	0.66
	0.1708	0.9209	300.21	194.75	0.9570	85.1164	0.0110	1.0111	0.936	0.12
303.15K	0	0.8001	187.25	95.74	1.4961	111.2926	0.0050	1.0050	0.960	0.69
	0.0717	0.8082	260.21	187.01	2.0802	128.3055	0.0049	1.0049	0.953	0.24
	0.1708	0.8193	351.26	220.36	2.8083	149.5134	0.0039	1.0039	0.954	0.13
308.15K	0	0.7222	260.76	167.20	1.8255	139.5046	0.0050	1.0050	0.956	0.15
	0.0717	0.7329	306.80	192.54	2.1479	150.4021	0.0045	1.0045	0.955	0.14
	0.1708	0.7478	413.06	225.53	2.8914	175.5389	0.0036	1.0036	0.958	0.08
313.15K	0	0.6211	288.19	176.83	1.7083	161.6221	0.0052	1.0052	0.955	0.12
	0.0717	0.6911	359.36	198.22	2.1302	178.7315	0.0043	1.0043	0.957	0.08
	0.1708	0.7092	476.18	231.80	2.8227	206.8152	0.0035	1.0035	0.960	0.06

o in (S cm².mol⁻¹), Λ_m in (S cm².mol⁻¹)

Table 6. Nano ZnSO₄ association constants, activation energy, enthalpies, and entropies of the association at various temperatures in the presence of trans hydroxyProline.

T (K)	X _s	E _a (kJ.mol ⁻¹)	ΔH _A (kJ.mol ⁻¹)	TΔS _A (kJ.mol ⁻¹)		ΔS _A (J.mol ⁻¹)
298.15	0	8.1295	87.9382	106.2524	356.3725	
	0.0717	5.9376	38.7256	60.2915		202.2189
	0.1708	5.6669	39.2658	61.7054		206.9611
303.15	0	8.1295	87.9382	112.0797		369.7169
	0.0717	5.9376	38.7256	59.7759		197.1828
	0.1708	5.6669	39.2658	61.7311		203.6324
308.15	0	8.1295	87.9382	110.5513		358.7582
	0.0717	5.9376	38.7256	61.5495		199.739
	0.1708	5.6669	39.2658	63.3060		205.4389
313.15	0	8.1295	87.9382	111.3421		355.5551
	0.0717	5.9376	38.7256	63.0788		201.4333
	0.1708	5.6669	39.2658	64.6338		206.3991

3.3. Isolation of metal complexes.

Chemical and physical approaches were used to create and characterize complexes of (H₂L) with Zn (II) metal ions. All solid complexes were purified. Tables provide metal complexes' elemental analysis results and physical properties (7, 8). The experimental and theoretical data comparison demonstrated that the isolated complexes' compositions were established using the proposed formula. Organic solvents could not dissolve any of the solid complexes; however, DMF and dimethyl sulfoxide (DMSO) could dissolve them efficiently.

Table 7. H₂L with metal complexes: elemental characterization and physical properties.

NO	Compound	Formula	M.Wt	Yield	color	m.p	Found (Calculated)		
							C	H	M
1	H ₂ L	C ₅ H ₉ NO ₃	131.131	80	white	275	45.80 (45.83)	(6.92) (6.94)	—
2	[Zn(L)(H ₂ O) ₂]	ZnC ₅ H ₁₁ NO ₅	230.534	80	Yellowish-white	>300	26.05 (26.1)	(4.81) (4.84)	28.36 (28.46)

Table 8. The most significant infrared bands for H₂L and related metal complexes

Compound	ν(OH)	ν(NH) _{as}	ν(C=O) _s	ν(C=O) _{as}	M-N	M-O
H ₂ L	3285	3138	1591	1399	---	---
[Zn(L)(H ₂ O) ₂]	3420	---	1584	1381	426	519

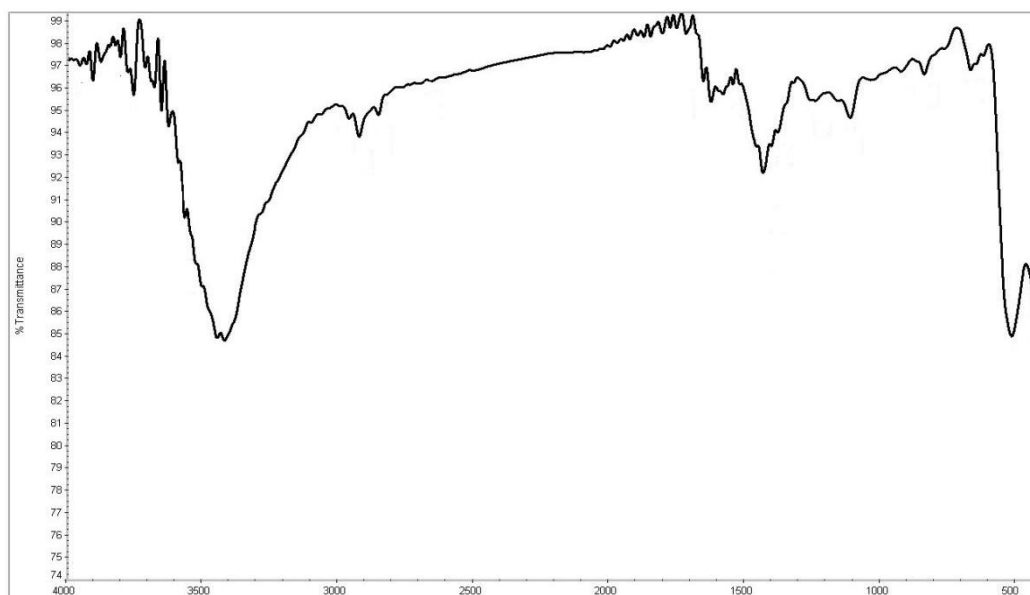


Figure 10. IR Spectrum of H₂L ligand.

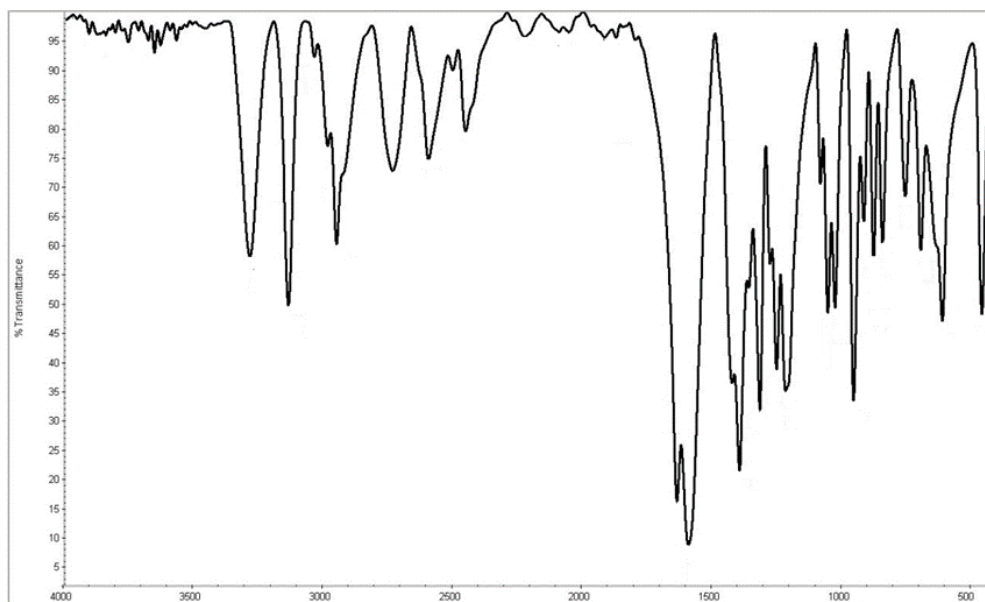


Figure 11. IR Spectrum of Zn(L)(H₂O)₂ complex.

3.4. Antimicrobial activity of H₂L and its metal complexes against *S. aureus*, *E. coli*, and *C. albicans*.

S. aureus, *E. coli*, and *C. albicans* were tested for H₂L antimicrobial properties and their metal complexes. The reference drugs are ampicillin (antibacterial) and clotrimazole (antifungal). Averaging the inhibitory zones of bacterial or fungal growth around each disc was calculated and presented as an average millimeter diameter [25-29]. From the obtained results for the diameter of the inhibition zone of Proline and its metal complexes, as illustrated in Fig, we concluded that most isolated complexes as zinc complexes have the largest antimicrobial activity. Complexes of Proline exhibited selectivity against G- bacteria as in the figure complex of Zn (II) has the most potent (84%) followed by Cu (II) (48%).

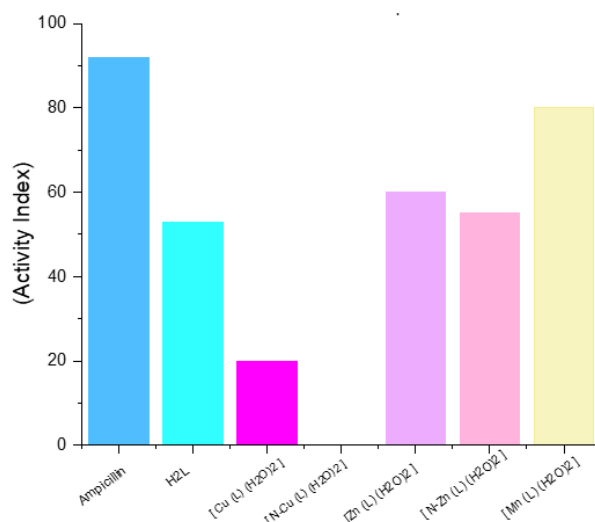


Figure 12. Effect of trans-4-Hydroxy-Proline and its metal complexes towards *E. coli*.

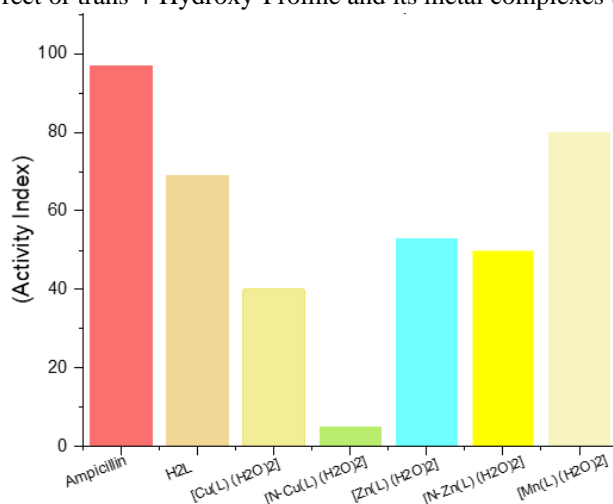


Figure 13. Effect of trans-Hydroxyl-Proline and its metal complexes towards *Staphylococcus aureus*.

H₂L showed an antibacterial effect against G⁺ bacteria for Zn (II) largest one (83.3%), followed by Cu (II) complex (58.2%) and nano Cu (II) complex (54.2%).

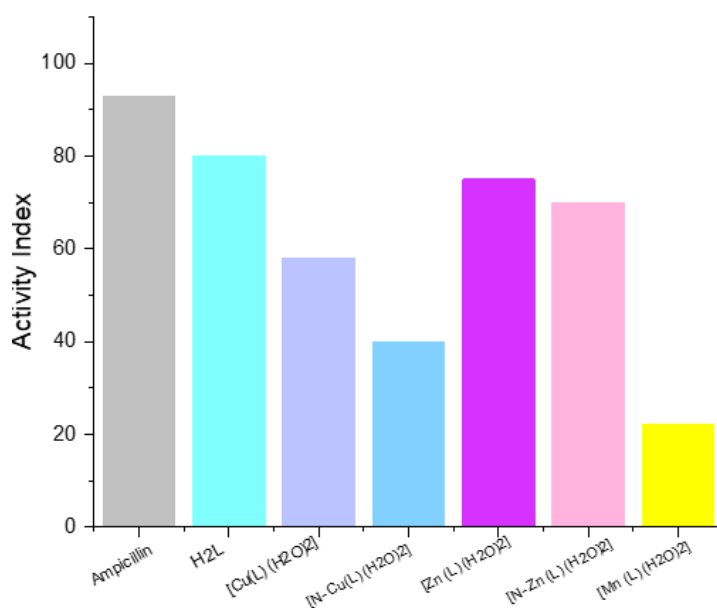


Figure 14. Effect of trans-4-Hydroxy-Proline and its metal complexes towards *C. albicans*.

Also displayed towards *C. albicans* that Cu (II) complex owes the most potent antibacterial (80.8%) followed by nano Cu (II) complexes (61.5%), but zinc complex has the lowest antibacterial effect towards *C. albicans*.

4. Conclusions

The association parameters for proline amino acid with nano ZnSO₄ are great values in all the pure and mixed (MeOH-H₂O) solvents used. This is because these values contain the association and favor complex formation. All calculated thermodynamic parameters for nano ZnSO₄ mainly association constants and Gibbs association energy, have great values and increase with an increase of the temperature due to the increase of mobility of ions in solutions. Similarly, the association values increase by increasing methanol percentage due to less solvation. The triple ion for association constants is very small in nano ZnSO₄ measurements.

Furthermore, the activity coefficient values increase by increasing temperatures indicating more ion-ion interactions, which support the increase in association parameters. The decrease in enthalpy of association ΔH_A for nano ZnSO₄ by increasing temperature indicates easier solvation at higher temperatures. The present study traces the development of Zn (II) complexes containing biologically significant ligands. In conjunction with data on the stability constants of such amino acid complexes.

Funding

This research received no external funding.

Acknowledgments

This research has no acknowledgment.

Conflicts of Interest

The authors declare no conflict of interest.

References

1. Gehlot, P.S.; Gupta, H.; Rathore, M.S.; Khatri, K.; Kumar, A. Intrinsic MRI contrast from amino acid-based paramagnetic ionic liquids. *Materials Advances* **2020**, *1*, 1980-1987, <https://doi.org/10.1039/D0MA00339E>.
2. Krishnamurthy, V.M.; Kaufman, G.K.; Urbach, A.R.; Gitlin, I.; Gudiksen, K.L.; Weibel, D.B.; Whitesides, G.M. Carbonic anhydrase as a model for biophysical and physical-organic studies of proteins and protein-ligand binding. *Chemical reviews* **2008**, *108*, 946-1051, <https://doi.org/10.1021/cr050262p>.
3. Gauthier-Coles, G.; Vennitti, J.; Zhang, Z.; Comb, W.C.; Xing, S.; Javed, K.; Bröer, A.; Bröer, S. Quantitative modelling of amino acid transport and homeostasis in mammalian cells. *Nature communications* **2021**, *12*, 1-18, <https://doi.org/10.1038/s41467-021-25563-x>.
4. Bagherani, N.; Smoller, B.R. An overview of zinc and its importance in dermatology-Part I: Importance and function of zinc in human beings. *Glob. Dermatol* **2016**, *3*, 330-336.
5. Zhang, S.-D.; Ma, P.-H.; Zhai, Y.-C.; Chen, W.-M. Determination of vanadyl sulfate ion-pair dissociation constant at 298.15 K by Fuoss method. *Rare Metals* **2015**, *34*, 873-876, <https://doi.org/10.1007/s12598-014-0353-9>.
6. Zhu, S.; Sun, W.; Wang, Q.; Yin, H.; Wang, B. Review of R&D status of vanadium redox battery. *Chemical industry and engineering progress* **2007**, *26*.
7. Rashad, R.; Gomaa, E. Thermodynamic Parameters for solvation of Copper sulphate in (ethanol-water) mixed solvent at different temperatures. *Asian Journal of Nanosciences and Materials* **2018**, *1*, 81-89.
8. Krężel, A.; Maret, W. The biological inorganic chemistry of zinc ions. *Archives of biochemistry and biophysics* **2016**, *611*, 3-19, <https://doi.org/10.1016/j.abb.2016.04.010>.

9. Trzaskowski, B.; Adamowicz, L.; Deymier, P.A. A theoretical study of zinc (II) interactions with amino acid models and peptide fragments. *JBIC Journal of Biological Inorganic Chemistry* **2008**, *13*, 133-137, <https://doi.org/10.1007/s00775-007-0306-y>.
10. Dizer, O.A.; Rogozhnikov, D.A.; Naboichenko, S.S. Thermodynamics of Copper Arsenious Raw Materials Dissolution in Nitric Acid. In: *Proceedings of the Solid State Phenomena*. **2021**; pp. 678-683, <https://doi.org/10.4028/www.scientific.net/SSP.316.678>.
11. Sharma, T.; Shah, S.S.; Bamezai, R.K. Thermodynamic and Spectroscopic Studies of Pentoxifylline in Aqueous Glucose/Lactose Solutions. *Journal of Solution Chemistry* **2021**, *50*, 1363-1390, <https://doi.org/10.1007/s10953-021-01123-1>.
12. Versaci, M.; Palumbo, A. Magnetorheological fluids: Qualitative comparison between a mixture model in the extended irreversible thermodynamics framework and an Herschel–Bulkley experimental elastoviscoplastic model. *International Journal of Non-Linear Mechanics* **2020**, *118*, <https://doi.org/10.1016/j.ijnonlinmec.2019.103288>.
13. Seyedi, Z.; Amooey, A.A.; Amouei, A.; Tashakkorian, H. Pentachlorophenol removal from aqueous solutions using Montmorillonite modified by Silane & Imidazole: kinetic and isotherm study. *J Environ Health Sci Eng* **2019**, *17*, 989-999, <https://doi.org/10.1007/s40201-019-00414-6>.
14. Gomaa, E.A.; Mousa, M.A.; Zaky, R.R.; Atia, F. Non isothermal association thermodynamic parameters (Conductometrically) for bulk and nano nickel sulfate in mixed EtOH–H₂O solvents. *Chem. Sci. Rev. Lett* **2014**, *3*, 1148-1162.
15. Gomaa, E.A.; Abou El-Leef, E.M.; Shalaby, K.S.; Salem, S.E. Thermodynamic Effect of Bulk and Nano-CuCl₂ Salts on Tenoxicam Using a Variety of Different Techniques. *Journal of Environments* **2014**, *1*, 44-53.
16. Gomaa, E.A.; Abu-Qarn, R.M. Ionic association and thermodynamic parameters for solvation of vanadyl sulfate in ethanol-water mixtures at different temperatures. *Journal of molecular liquids* **2017**, *232*, 319-324, <http://dx.doi.org/10.1016/j.molliq.2017.02.085>.
17. Gomaa, E.A.; El-Defraway, M.M.; Hussien, S.Q. Estimation of cyclic voltammetry data for SrCl₂, CaCl₂ and their interaction with ceftriaxone sodium salt in KNO₃ using palladium working electrode. *European Journal of Advanced Chemistry Research* **2020**, *1*, <https://doi.org/10.24018/EJCHEM.2020.1.5.18>.
18. El-Shereafy, S.; Gomaa, E.; Yousif, A.; Abou Elyazed, A. Electrochemical and thermodynamic estimations of the interaction parameters for bulk and nano-silver nitrate (NSN) with cefdinir drug using a glassy carbon electrode. *Iranian Journal of Materials Science and Engineering* **2017**, *14*, 48-57, <http://dx.doi.org/10.22068/ijmse.14.4.48>.
19. Abou Elleef, E.M.; Abd El-Hady, M.N.; Gomaa, E.A.; Al-Harazie, A.G. Conductometric Association Parameters for CdBr₂ in the Presence and Absence of Ceftazidime in Water and 30% Ethanol–Water Mixtures. *Journal of Chemical & Engineering Data* **2021**, *66*, 878-889, <https://doi.org/10.1021/acs.jced.0c00150>.
20. Helmy, E.T.; Gomaa, E.A.; Abou Eleef, E.M. Gibbs free energy and activation free energy of complexation of some divalent cations with ampicillin in methanol at different temperatures. *American Journal of Applied Chemistry* **2016**, *4*, 256-259.
21. Equil, B.V.-L. Data. Available online: <https://www.cheric.org/research/kdb/hcvle/showvle.php?vleid=3848>. (accessed on 27 August **2021**).
22. Crea, F.; De Stefano, C.; Gigliuto, A.; Irto, A. Behavior of Antibacterial Ofloxacin; Hydration Constants and Solubility in Aqueous Solutions of Sodium Chloride at Different Temperatures. *Journal of Solution Chemistry* **2021**, *50*, 1236-1257, <https://doi.org/10.1007/s10953-021-01114-2>.
23. Abendrot, M.; Pluciennik, E.; Felczak, A.; Zawadzka, K.; Piątczak, E.; Nowaczyk, P.; Kalinowska-Lis, U. Zinc (II) Complexes of Amino Acids as New Active Ingredients for Anti-Acne Dermatological Preparations. *International journal of molecular sciences* **2021**, *22*, <https://doi.org/10.3390/ijms22041641>.
24. Begum, J.S.; Manjunath, K.; Pratibha, S.; Dhananjaya, N.; Sahu, P.; Kashaw, S. Bioreduction synthesis of zinc oxide nanoparticles using Delonix regia leaf extract (Gul Mohar) and its agromedicinal applications. *Journal of Science: Advanced Materials and Devices* **2020**, *5*, 468-475, <https://doi.org/10.1016/j.jsamd.2020.07.009>.
25. Pal, J.; Patla, A.; Subramanian, R. Thermodynamic properties of forming methanol-water and ethanol-water clusters at various temperatures and pressures and implications for atmospheric chemistry: A DFT study. *Chemosphere* **2021**, *272*, <https://doi.org/10.1016/j.chemosphere.2021.129846>.
26. Refat, H.M.; Fadda, A. Synthesis and antimicrobial activity of some novel hydrazide, benzochromenone, dihydropyridine, pyrrole, thiazole and thiophene derivatives. *European journal of medicinal chemistry* **2013**, *70*, 419-426, <https://doi.org/10.1016/j.ejmech.2013.09.003>.
27. Zaky, R.; Yousef, T.; Ibrahim, K. Co (II), Cd (II), Hg (II) and U (VI) O₂ complexes of o-hydroxyacetophenone [N-(3-hydroxy-2-naphthoyl)] hydrazone: Physicochemical study, thermal studies and antimicrobial activity. *Spectrochimica Acta Part A: Molecular and Biomolecular Spectroscopy* **2012**, *97*, 683-694, <https://doi.org/10.1016/j.saa.2012.05.086>.
28. Thakur, R. Study On Transport Phenomenon Of Some Divalent Transition Metal Sulphates And Magnesium Sulphate In Binary Aqueous Mixtures Of Diethylene Glycol (Deg). *Plant Archives* **2020**, *20*, 3083-3088.

29. Sandhiyapriya, T.; Muneeswari, K.; Gomathi, M.; Shanmugarathinam, A.; Akshay, S.; Ahamed, M.I.N. Antibacterial and Antifungal Activity of Cadmium Sulphide Nanoparticles. *Annals of the Romanian Society for Cell Biology* **2021**, *25*, 4209-4218.